Physics Letters B 729 (2014) 9–14

Contents lists available at ScienceDirect

Physics Letters B

www.elsevier.com/locate/physletb

Identification of non-ordinary mesons from the dispersive connection between their poles and their Regge trajectories: The $f_0(500)$ resonance

J.T. Londergan [a,b], J. Nebreda [a,b,c,d], J.R. Pelaez [c,*], A.P. Szczepaniak [a,b,e]

[a] Center for Exploration of Energy and Matter, Indiana University, Bloomington, IN 47403, USA
[b] Department of Physics, Indiana University, Bloomington, IN 47405, USA
[c] Departamento de Física Teórica II, Universidad Complutense de Madrid, 28040 Madrid, Spain
[d] Yukawa Institute for Theoretical Physics, Kyoto University, 606-8502 Kyoto, Japan
[e] Jefferson Laboratory, 12000 Jefferson Avenue, Newport News, VA 23606, USA

ARTICLE INFO

Article history:
Received 7 August 2013
Received in revised form 30 December 2013
Accepted 30 December 2013
Available online 31 December 2013
Editor: J.-P. Blaizot

Keywords:
Regge theory
Light scalar mesons

ABSTRACT

We show how the Regge trajectory of a resonance can be obtained from its pole in a scattering process and analytic constraints in the complex angular momentum plane. The method is suited for resonances that dominate an elastic scattering amplitude. In particular, from the $\rho(770)$ resonance pole in $\pi\pi$ scattering, we obtain its linear Regge trajectory, characteristic of ordinary quark–antiquark states. In contrast, the $f_0(500)$ pole—the sigma meson—which dominates scalar isoscalar $\pi\pi$ scattering, yields a nonlinear trajectory with a much smaller slope at the $f_0(500)$ mass. Conversely, imposing a linear Regge trajectory for the $f_0(500)$, with a slope of typical size, yields an elastic amplitude at odds with the data. This provides strong support for the non-ordinary nature of the sigma meson.

1. Introduction

There is growing evidence for the existence of hadrons that fall beyond the ordinary quark–antiquark classification of mesons or three quark classification of baryons.

Most current investigations of dynamical models underlying resonance formation focus on individual partial waves. This allows to study poles of amplitudes in the complex energy plane at fixed angular momentum and their spectroscopic classification into SU(3) multiplets, which by itself provides limited information about their composition. In this work we take advantage of the analytical properties of amplitudes in the complex angular momentum plane and this enables us to investigate the dynamical linkage of resonances of different spins. The function connecting such resonances is known as the Regge trajectory and its form can be used to discriminate between the underlying (QCD) mechanisms responsible for generating the resonances. For example, linear (J, M^2) trajectories relating the angular momentum J and the mass squared are naively and intuitively interpreted in terms of the rotation of the flux tube connecting a quark and an antiquark. Strong deviations from this linear behavior would suggest a rather different nature.

For illustration, we will apply our method to light resonances in elastic $\pi\pi$ scattering. We consider the $\rho(770)$, which suits well the ordinary meson picture, and also the $f_0(500)$ or σ meson, whose nature, spectroscopic classification, and even its existence have been the subject of a longstanding debate. Apart from its significant role in our understanding of the spontaneous chiral symmetry breaking of QCD, the nucleon–nucleon attraction, or even the identification of the lightest glueball, our interest in the $f_0(500)$ is that different approaches [1,2] suggest that it may not be an ordinary quark–antiquark meson. Furthermore, the σ meson is often omitted from (J, M^2) trajectory fits [3], since it does not "fit well into this classification" or, as in [4], because it has a large width and it contributes little to the χ^2, but was included in the n-trajectories.

The input for our approach is just the position and residue of the resonance poles in $\pi\pi$ scattering. Our $f_0(500)$ choice is then even more pertinent, because for long its pole parameters have been plagued by systematic uncertainties. However, recent and rigorous dispersive analyses on scattering data have provided a model-independent and accurate determination of the $f_0(500)$ [5,6], finally settling [7] the controversy on its existence.

Even though we shall not be able to compute trajectories over a large energy range, the local behavior can be quite telling. In practice we aim at obtaining the slope and the intercept of the Regge

* Corresponding author.

http://dx.doi.org/10.1016/j.physletb.2013.12.061

trajectory where the $f_0(500)$ lies, showing the striking differences with the $\rho(770)$, thus explaining why it does not fit into the ordinary linear trajectory classification.

This work focuses on properties of Regge poles of the scattering amplitude. In this context, our working definition of an ordinary meson is that it corresponds to a pole which lies on a Regge trajectory that is almost real and linear with slope of the order of 1 GeV^{-2}. We show that the Regge trajectory of the $\rho(770)$ satisfies this criterion, while that of the $f_0(500)$ does not. Since trajectories of ordinary mesons are qualitatively understood in terms of conventional quark–antiquark dynamics, the fact that the $f_0(500)$ trajectory is different suggests that a different mechanism is responsible for the formation of the $f_0(500)$, although at present we cannot specify what that mechanism might be.

2. Regge trajectory from a single pole

Let us recall that within analytic S-matrix theory, the method of imposing unitarity constraints from the crossed channels on the direct channel is that of analytic continuation of partial waves into the complex angular momentum plane. Singularities in the angular momentum plane, *e.g.* Regge poles, interpolate between direct and crossed-channel dynamics, containing the most complete description of resonance parameters.

2.1. Analytic constraints on the trajectory and the residue

An elastic $\pi\pi$ partial wave near a Regge pole reads

$$t_l(s) = \beta(s)/\big(l - \alpha(s)\big) + f(l,s), \tag{1}$$

where $f(l,s)$ is a regular function of l, whereas the Regge trajectory $\alpha(s)$ and residue $\beta(s)$ satisfy $\alpha(s^*) = \alpha^*(s)$, $\beta(s^*) = \beta^*(s)$, in the complex-s plane cut along the real axis for $s > 4m_\pi^2$. Note that the pole appears in the second Riemann sheet of $t_l(s)$, which we normalize as

$$t_l(s) = e^{i\delta_l(s)} \sin\delta_l(s)/\rho(s), \quad \rho(s) = \sqrt{1 - 4m_\pi^2/s} \tag{2}$$

with $\delta_l(s)$ being the phase shift. Now, if the pole dominates in Eq. (1), the unitarity condition above threshold $\operatorname{Im} t_l(s) = \rho(s)|t_l(s)|^2$ analytically continued to complex l implies that, for real l,

$$\operatorname{Im}\alpha(s) = \rho(s)\beta(s). \tag{3}$$

For integer-l partial waves the unitarity relation gives the prescription for how to analytically continue $t_l(s)$ below the elastic cut for $s > 4m_\pi^2$. Similarly, Eq. (3) determines the continuation of $\alpha(s)$, which we will use when studying resonance poles that occur at fixed, integer l and complex s.

Note that, if $\beta(s)$ was known, we could use a dispersion relation to determine $\alpha(s)$. Therefore we first discuss the analytic properties of the former [8]. Near threshold, partial waves behave as $t_l(s) \propto q^{2l}$, where $q^2 = s/4 - m_\pi^2$ and thus, $\beta(s) \propto q^{2\alpha(s)}$. Moreover, since the Regge pole contribution to the full amplitude is proportional to $(2\alpha+1)P_\alpha(z_s)$, where z_s is the s-channel scattering angle, in order to cancel poles of the Legendre function $P_\alpha(z_s) \propto \Gamma(\alpha + 1/2)$ the residue has to vanish when $\alpha + 3/2$ is a negative integer, i.e.,

$$\beta(s) = \gamma(s)\hat{s}^{\alpha(s)}/\Gamma\big(\alpha(s) + 3/2\big), \tag{4}$$

where $\hat{s} = (s - 4m_\pi^2)/s_0$. The dimensional scale $s_0 = 1$ GeV^2 is introduced for convenience and the reduced residue $\gamma(s)$ is, once again, a real analytic function. Since on the real axis $\beta(s)$ is real, the phase of γ is

$$\arg\gamma(s) = -\operatorname{Im}\alpha(s)\log(\hat{s}) + \arg\Gamma\big(\alpha(s) + 3/2\big). \tag{5}$$

Analyticity therefore demands that

$$\gamma(s) = P(s)\exp\left(c_0 + c's + \frac{s}{\pi}\int_{4m_\pi^2}^{\infty} ds' \frac{\arg\gamma(s')}{s'(s'-s)}\right), \tag{6}$$

where $P(s)$ is an entire function. Given that we use the elastic approximation, the behavior at large s cannot be determined from first principles. However as we expect linear Regge trajectories to emerge for the $\rho(770)$, we should allow α to behave as a first order polynomial at large-s. This implies that $\operatorname{Im}\alpha(s)$ decreases with growing s and thus $\alpha(s)$ obeys the dispersion relation [9],

$$\alpha(s) = \alpha_0 + \alpha' s + \frac{s}{\pi}\int_{4m_\pi^2}^{\infty} ds' \frac{\operatorname{Im}\alpha(s')}{s'(s'-s)}. \tag{7}$$

To match the asymptotic behavior of $\beta(s)$ and $\operatorname{Im}\alpha(s)$ (assuming $\alpha' \neq 0$), it follows from the unitarity equation, Eq. (3), that $c' = \alpha'(\log(\alpha' s_0) - 1)$ and that $P(s)$ can at most be a constant. Hence, together with Eq. (1), the following three equations define the "constrained Regge-pole" amplitude [8]:

$$\operatorname{Re}\alpha(s) = \alpha_0 + \alpha' s + \frac{s}{\pi} PV \int_{4m_\pi^2}^{\infty} ds' \frac{\operatorname{Im}\alpha(s')}{s'(s'-s)}, \tag{8}$$

$$\operatorname{Im}\alpha(s) = \frac{\rho(s) b_0 \hat{s}^{\alpha_0+\alpha' s}}{|\Gamma(\alpha(s) + \frac{3}{2})|}\exp\left(-\alpha' s\big[1 - \log\big(\alpha' s_0\big)\big] + \frac{s}{\pi} PV \times \int_{4m_\pi^2}^{\infty} ds' \frac{\operatorname{Im}\alpha(s')\log\frac{\hat{s}}{\hat{s}'} + \arg\Gamma(\alpha(s') + \frac{3}{2})}{s'(s'-s)}\right), \tag{9}$$

$$\beta(s) = \frac{b_0 \hat{s}^{\alpha_0+\alpha' s}}{\Gamma(\alpha(s) + \frac{3}{2})}\exp\left(-\alpha' s\big[1 - \log\big(\alpha' s_0\big)\big] + \frac{s}{\pi}\int_{4m_\pi^2}^{\infty} ds' \frac{\operatorname{Im}\alpha(s')\log\frac{\hat{s}}{\hat{s}'} + \arg\Gamma(\alpha(s') + \frac{3}{2})}{s'(s'-s)}\right), \tag{10}$$

where PV denotes "principal value". Note that Eqs. (9) and (10) reduce to Eq. (3) for real s.

For the σ-meson, $\beta(s)$ at low energies should also include the Adler-zero required by chiral symmetry. In practice it is enough to place it at the leading order chiral perturbation theory result [12], i.e., $\beta(s) \propto 2s - m_\pi^2$. This should be done without spoiling the large s-behavior, which can be achieved by replacing $\Gamma(\alpha + 3/2)$ by $\Gamma(\alpha + 5/2)$. Such modification leaves the pole at $\alpha(s) = -3/2$ uncanceled. This is not an issue since for the σ trajectory, $\alpha(s) = \alpha_\sigma(s)$ this pole will be located far outside the range of applicability of our approach. Hence, for the $f_0(500)$ we should just multiply the right hand side of Eq. (9) by $2s - m_\pi^2$ and replace the 3/2 by 5/2 inside the gamma functions. Note that b_0 now is not dimensionless.

2.2. Numerical analysis

We solve the equations for $\alpha(s)$ and $\beta(s)$ numerically. The only inputs are the pole positions s_M and residues $|g_M|$ for the $M = \rho(770)$ and the $f_0(500)$ resonances. Specifically, the poles are

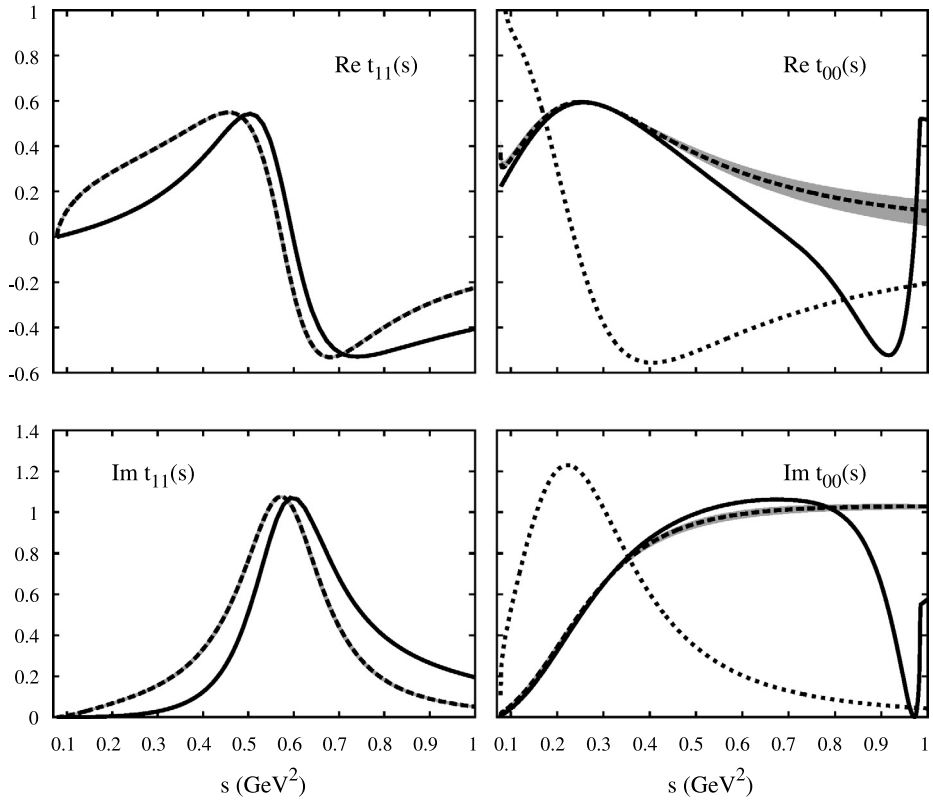

Fig. 1. Partial waves t_{Il} (I being the isospin) with the $l=1$ wave shown in the left and $l=0$ in the right panels, respectively. Solid lines represent the amplitudes from [10]. The resonance poles of these amplitudes [6] determine the constrained Regge-pole amplitudes shown with dashed curves. The estimated systematic uncertainties are shown as gray bands (almost indistinguishable from the dashed line in the case of t_{11}). In the right panels, the dotted lines represent the constrained Regge-pole amplitude for the S-wave if the σ-pole is fitted by imposing a linear trajectory with $\alpha' \simeq 1$ GeV^{-2}.

used as input for determining the α_0, α', b_0 parameters of the corresponding Regge trajectories, by requiring that at the pole, on the second Riemann sheet, $\beta_M(s)/(l-\alpha_M(s)) \to |g_M^2|/(s-s_M)$, with $l=0,1$ for $M=\sigma,\rho$. We minimize the sum of the squared differences between the input and output values for the real and imaginary parts of the pole position and for the absolute value of the squared coupling, divided by the corresponding squared uncertainties. The pole parameters are taken from a precise dispersive representation of $\pi\pi$ scattering data [6,10] that enables a model independent, analytic continuation of partial wave amplitudes to the complex energy plane.

For a given set of α_0, α' and b_0 parameters we solve the system of Eqs. (8) and (9), with the modification due to the Adler-zero in the scalar case, as discussed above. This is done by setting $\mathrm{Im}\,\alpha(s)=0$ initially, which yields $\mathrm{Re}\,\alpha(s)$ using Eq. (8). Then, these real and imaginary parts of α are used in Eq. (9) to obtain $\mathrm{Im}\,\alpha(s)$. This process is iterated until the results converge. Thus, we obtain a constrained Regge-pole amplitude, under the approximation that it is dominated by a single Regge trajectory. This amplitude, determined by a pole at a given complex s and real l, can be extended to any value in the complex s-plane. In particular we can compare this Regge amplitude on the real axis with the partial waves of [10]. The two amplitudes do not have to overlap on the real axis since they are only constrained to agree at the resonance pole.

The left panels of Fig. 1 show the real and imaginary parts of the P wave. The solid curves give the Constrained Data Fits of [10] whose $\rho(770)$ pole position, $\sqrt{s_\rho} = 763.7^{+1.7}_{-1.5} - i73.2^{+1.0}_{-1.1}$ MeV and residue, $|g_\rho| = 6.01^{+0.04}_{-0.07}$ [6] were used as input. As discussed above, these are then fit with Eq. (1) for $l=1$, where $\alpha(s)$ and $\beta(s)$ satisfy the coupled Eqs. (8) and (9). The output values for the fitted pole are: $\sqrt{s_\rho} = 762.7 - i73.5$ MeV and $|g_\rho| = 5.99$. The resulting real and imaginary parts of this Regge-pole amplitude on the real axis are shown as dashed lines in the left column of Fig. 1. The gray bands cover the uncertainties due to the errors in the determination of the pole positions and residues from the dispersive analysis of data in [10]. In the resonant region there is fair agreement between our resulting amplitude and that from [10]. The ρ peak is clearly identified in the imaginary part, and, as expected, the agreement deteriorates as we approach threshold or the inelastic region, where the pole is less dominant.

The right panels of Fig. 1 display the S wave from [10] (solid curves), with a pole [6] at $\sqrt{s_\sigma} = 457^{+14}_{-13} - i279^{+11}_{-7}$ MeV and residue $|g_\sigma| = 3.59^{+0.11}_{-0.13}$ GeV. Dashed lines correspond to the Regge-pole partial wave, whose pole is at $\sqrt{s_\sigma} = 461 - i281$ MeV and $|g_\sigma| = 3.51$ GeV. It is well known that the $f_0(500)$ does not conform to a Breit–Wigner shape but still dominates the partial wave from threshold up to almost 1 GeV, where it strongly interferes with the very narrow $f_0(980)$. We find a remarkably good agreement between our input and output amplitudes from threshold up to 0.5 GeV^2, where the agreement starts to deteriorate.

Since our constrained Regge amplitudes provide a fair representation of the resonance region, we show in Fig. 2 the resulting Regge trajectories. We see that the imaginary part of $\alpha_\rho(s)$ is much smaller than the real part. In addition, the latter grows linearly with s, with intercept $\alpha_\rho(0) = 0.520 \pm 0.002$. Note that the error band we provide is only due to the uncertainty in the input pole parameters from Ref. [6].

This value for the intercept is consistent with that obtained from the extensive study [3] of (J, M^2) resonance trajectories. It can also be compared with $\alpha_\rho(0) = 0.52 \pm 0.02$ from fits to total cross sections for NN, πN and $\pi\pi$ [11], or to the value of $\alpha_\rho(0) = 1 - \eta_2 = 0.450 \pm 0.005$ [7], which includes an even

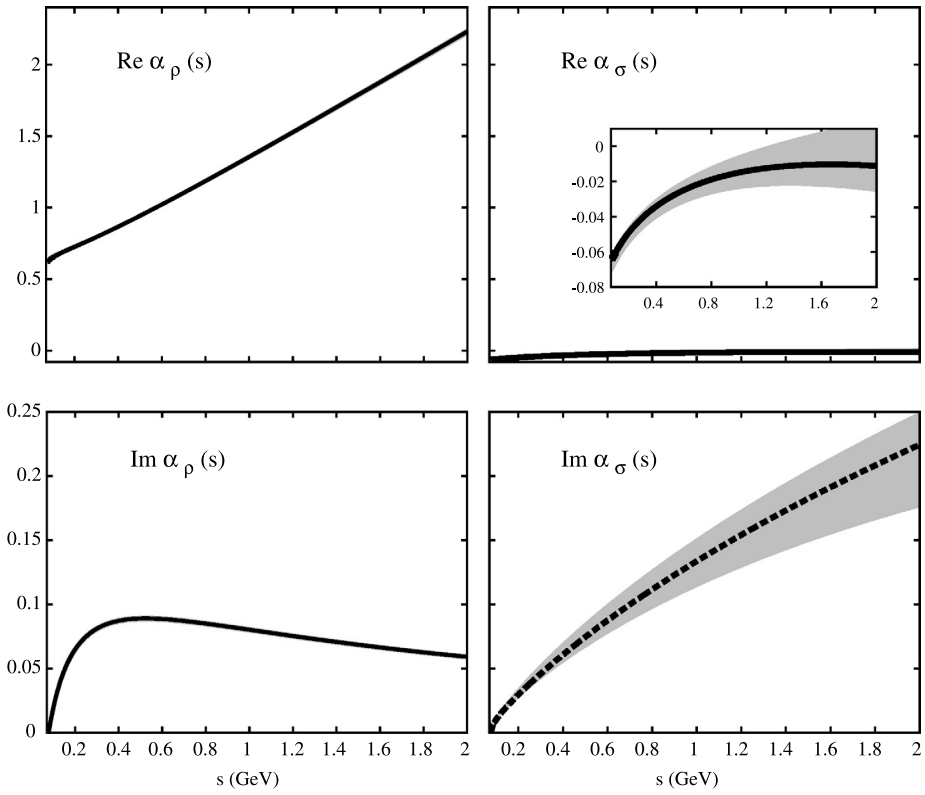

Fig. 2. Real and imaginary parts of the resonance Regge trajectory obtained from the resonance pole parameters as explained in the text. The $\rho(770)$ trajectory shown in the left panel is almost real and linearly rising. In the right panel, we observe that real and imaginary parts of the $f_0(500)$ trajectory are comparable with the former having a much smaller slope than that of the ρ.

larger number of channels. Moreover, the resulting slope $\alpha'_\rho = 0.902 \pm 0.004\ \text{GeV}^{-2}$ is consistent with fits of a linear trajectory to the $\rho(770)$, $\rho_3(1690)$ and $\rho_5(2350)$ mesons performed in [3] and more recently in [4] that yield $\alpha'_\rho \simeq 0.83\ \text{GeV}^{-2}$ and $\alpha'_\rho \simeq 0.87 \pm 0.06\ \text{GeV}^{-2}$, respectively. A value of $\alpha'_\rho = 0.9\ \text{GeV}^{-2}$ was used in [11].

Taking into account our approximations, and that our error bands only reflect the uncertainty in the input pole parameters, our results are in remarkable agreement with trajectories from the literature and provide a benchmark of the validity of our approach.

Regarding the $f_0(500)$ trajectory shown in the right panel of Fig. 2, we see that it is evidently nonlinear. We obtain

$$\alpha_\sigma(0) = -0.090^{+0.004}_{-0.012}, \qquad \alpha'_\sigma \simeq 0.002^{+0.050}_{-0.001}\ \text{GeV}^{-2},$$

where, once again, the error bands are due to the uncertainty in the input pole parameters from [6]. The slope is about two orders of magnitude smaller than that of the ρ (and other trajectories typical to quark–antiquark resonances, *e.g.* a_2, f_2, π_2). This provides strong support for a non-ordinary nature of the σ meson. Furthermore the growth of $\alpha_\sigma(s)$ is so slow that it excludes the possibility that any of the known isoscalar resonances $f_2, f_4, \ldots$ lie on the σ meson trajectory. Our result therefore explains why the $f_0(500)$ does not fit well in the usual hadron classification into linear trajectories with a slope of typical hadronic size.

To show the difference between the $\rho(770)$ and $f_0(500)$ trajectories, in the left panel of Fig. 3 we plot both the real and imaginary parts of the two trajectories using the same scale. Not only is the difference clearly evident between the shape and magnitude of the real part of the $\rho(770)$ trajectory and that of the $f_0(500)$, but also the fact that the real and imaginary parts of the $f_0(500)$ trajectory are comparable.

Furthermore, in Fig. 3 we show the striking similarities between the $f_0(500)$ trajectory and those of Yukawa potentials in non-relativistic scattering, not only at low energies below $s = 2\ \text{GeV}^2$, represented by the thick continuous line, but also when extrapolated beyond that energy, which we show as a thick dashed–dotted line that describes a backward loop in the complex plane before moving to infinity. Of course, our results are most reliable at low energies and the extrapolation should be interpreted cautiously. Nevertheless, our results suggest that the $f_0(500)$ looks more like a low-energy resonance of a short range potential, *e.g.* between pions, than a bound state of a long range confining force between a quark and an antiquark.

Concerning the uncertainties in the input parameters [6], we observe that from threshold energies up to $s = 2\ \text{GeV}^2$, i.e., the gray band around the thick continuous line, all trajectories bear a close similarity to Regge trajectories of Yukawa potentials as it happens for the central curve. Of course, when extrapolating our results to higher energies, the uncertainty band becomes larger. Most of the trajectories we find within the uncertainties still describe a loop in the $(\text{Re}\,\alpha, \text{Im}\,\alpha)$ plane, but a few of them describe a trajectory where the loop has collapsed (these are represented by a somewhat darker gray band). For the latter the $\alpha' s$ term is somewhat stronger and it prevents formation of a loop. Below $s = 2\ \text{GeV}^2$, all trajectories follow a qualitative behavior similar to that of a Yukawa potential and even when extrapolated to higher energies they do *not* follow an ordinary almost-real linear Regge trajectory with a slope of order 1 GeV^{-2}.

One could also wonder if the weak $f_0(500)$ trajectory is affected by other uncertainties, hidden in the neglected background amplitude (*cf.* Eq. (1)). If we try to fit the pole in [10] by fixing α' to a more natural value, say the one for the $\rho(770)$, we obtain a χ^2 which is two orders of magnitude larger, with the

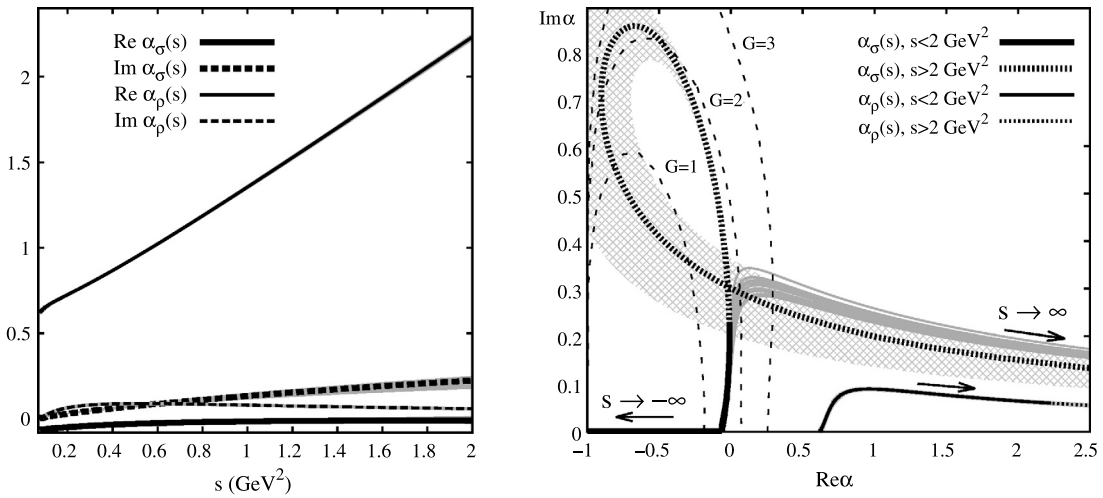

Fig. 3. (Left) $\alpha_\rho(s)$ and $\alpha_\sigma(s)$ Regge trajectories, from our constrained Regge-pole amplitudes. The ρ trajectory is almost real and linear, whereas both the real and imaginary parts of $\alpha_\sigma(s)$ are very small, and not evidently linear. For the error bands we use the same convention as in Fig. 1. In most cases the bands are so thin that they are barely distinguishable from the central lines. (Right) $\alpha_\sigma(s)$ and $\alpha_\rho(s)$ in the complex plane. Beyond $s = 2$ GeV^2 extrapolations of our results are plotted as dotted lines. Asymptotically, i.e., $s > 200$ GeV^2, the small real part, proportional to $\alpha' s$ takes over the dispersive contribution and $\mathrm{Re}\,\alpha_\sigma(s)$ starts growing, similar to $\mathrm{Re}\,\alpha_\rho(s)$. Within the input pole parameter error bands, in the case of the σ, we find two types of solutions for the trajectory. One set has a loop in the $\mathrm{Im}\,\alpha - \mathrm{Re}\,\alpha$ plane. The other, having slightly higher α' does not form a loop. The pattern-filled band encloses the first type of solutions, whereas the gray lines correspond to the other set. At low and intermediate energies, both are similar to the trajectories of the Yukawa potential $V(r) = -Ga\exp(-r/a)/r$, shown here for three different values of G [13]. For the G = 2 Yukawa curve to reach the value of $\mathrm{Im}\,\alpha = 0.23$ at $s = 2$ GeV^2, as our curve does, we can estimate $a \simeq 0.5$ GeV^{-1}, following [13]. This could be compared, for instance, to the S-wave $\pi\pi$ scattering length $\simeq 1.6$ GeV^{-1}.

pole at $\sqrt{s_\sigma} = 487 - i199$ MeV and a much larger coupling $|g_\sigma| = 4.09$ GeV. Even worse, as seen by the dotted curve in the right panel of Fig. 1, on the real axis the real and imaginary parts of the resulting Regge-pole amplitude are qualitatively different from the expected behavior for the S-wave. We note that this exercise is also highly relevant because it illustrates that the large resonance width is not responsible for the fact that the $f_0(500)$ does not follow an ordinary Regge trajectory.

Finally we show the results obtained for the $f_0(500)$ trajectory when using the unmodified dispersion relation of Eq. (9) instead of the one in which the Adler zero has been fixed. In this case the pole position and coupling can be reproduced fairly well: $\sqrt{s_\sigma} = 476 - i280$ MeV, $|g_\sigma| = 3.20$ GeV (although with a χ^2 still 20 times larger than that of the fit with the modified dispersion relation). However, the corresponding amplitude on the real energy axis turns out to be completely different from that of the dispersive analysis, and consequently does not agree with the experimental data. This is apparent in the left panel of Fig. 4. In addition, in the right panel of Fig. 4 we show the real and imaginary parts of its Regge trajectory. The results are quite similar to the case when we do not factor out the Adler zero. Actually, both are once again completely flat compared to the real part of the ρ trajectory (to ease the comparison, the same scale as that of Fig. 3 has been used for the real part). The parameters of this trajectory are: $\alpha_0 = -0.002$ and $\alpha' = 0.015$ GeV^{-2}, once again very different from the corresponding values for ordinary meson trajectories. It seems that the Adler zero is quite important to obtain a reasonable description of data, but is not responsible for the non-ordinary behavior of the $f_0(500)$, which seems to be mainly determined by values of the pole parameters, i.e., the mass, width and residue.

3. Summary and discussion

To summarize, we have shown how to obtain the Regge trajectory of a light resonance from its associated pole, when that dominates the elastic scattering of two hadrons. The method is based on general analytic properties and yields a set of integral relations for the Regge trajectory and its residue. These are solved iteratively while fitting just the pole position and coupling of the given resonance. The method works fairly well for the $\rho(770)$, which dominates elastic $\pi\pi$ vector–isovector scattering. The resulting trajectory is almost real and nearly linear. Given our approximations, the intercept and slope come remarkably close to values in the literature, obtained from fits to high energy scattering or to linear trajectories including the $\rho(770)$, $\rho_3(1690)$ and $\rho_5(2350)$. Our method thus identifies the $\rho(770)$ and its trajectory partners as ordinary mesons. It is worth noting that, since higher resonances are not included in the input, our method "predicts" such a tower of resonances, from just the pole and residue of the $\rho(770)$. Note that the method does not build in a nearly real and linear behavior.

The main objective of this Letter, however, was to estimate the Regge trajectory and residue of the σ or $f_0(500)$ scalar meson, whose pole position has been accurately determined by several groups using model independent dispersive techniques. Our estimate is relevant because the σ has been long considered a non-ordinary meson and is often excluded from linear Regge fits with slopes of typical hadronic size, $\simeq 1$ GeV^{-2}.

For the scalar case our method is modified to include the Adler zero required by chiral symmetry. We fit the pole and coupling obtained from dispersive studies of $\pi\pi$ scattering and obtain the Regge residue and trajectories. The resulting trajectory is more than one order of magnitude weaker than that of the ρ or any ordinary trajectory, and at low energies bears striking similarities with the trajectories of Yukawa potentials. The resulting scale of tens of MeV or at most hundreds, for the slope, is more typical of meson physics than of quark–antiquark interactions. The σ Regge trajectory is so flat that any trajectory partners would have to be extremely massive. To test the robustness of this observation we have checked that our results are very stable within the uncertainties of the pole parameters that we used as input. In addition we have tried to impose a typical size linear trajectory on the σ, but that deteriorates the fit to the σ pole and particularly to the coupling, so the resulting amplitude in the physical region is qualitatively very different from the observations. Therefore, the smallness of our estimate of the σ trajectory is robust

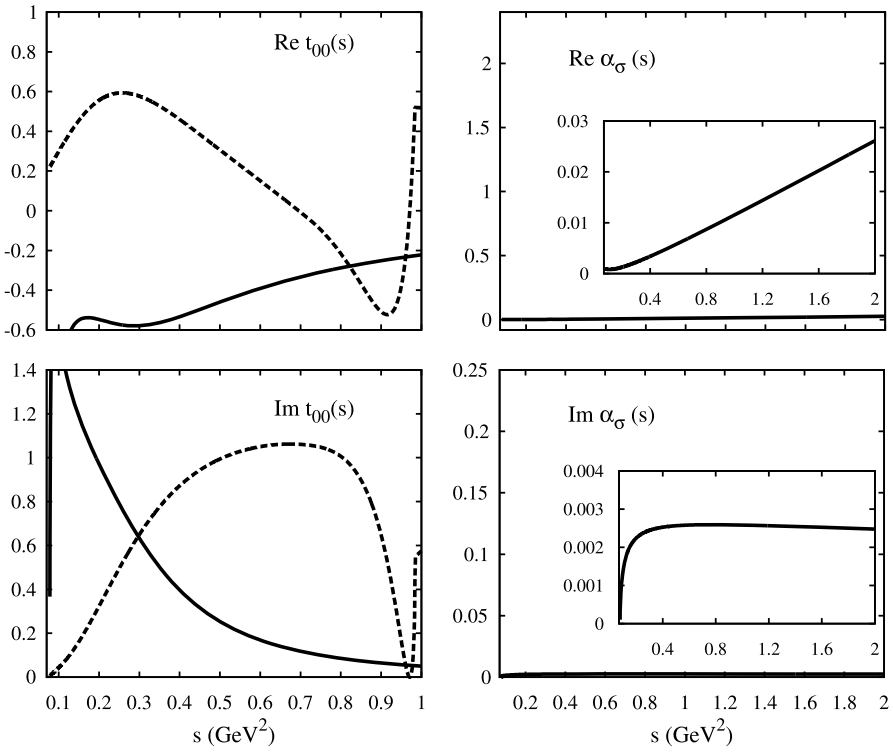

Fig. 4. Left panel: Dashed lines represent real (top) and imaginary (bottom) parts of the dispersive data analysis in [10] which provide the ρ and $f_0(500)$ poles [6]. These poles have been fitted here with the coupled dispersion relations of Eqs. (8) and (9), in which the Adler zero has not been imposed. The resulting real and imaginary parts of this Regge-pole amplitude are shown as black lines. Although the pole parameters are acceptably fitted, the amplitude in the real axis does not agree at all with that of the dispersive data analysis. Right panel: real (top) and imaginary (bottom) parts of the corresponding Regge trajectory.

and explains why it does not fit well in the usual Regge classification and strongly supports a non-ordinary nature of the lightest scalar meson.

Our method can be applicable to other resonances that dominate elastic scattering and generalization to inelastic channels is also straightforward. Hence we plan on studying the $K^*(892)$ vector and the $K(800)$ (or κ) scalar resonance, and possibly other meson–nucleon resonances. Furthermore we also plan on studying the N_c or quark mass dependence of the Regge trajectories and to explore hadronic resonance models that could explain this non-ordinary behavior (*e.g.*, tetraquarks, hadron molecules, etc.). We expect that this method should provide further understanding of the most controversial states in the hadron spectrum.

Acknowledgements

J.R.P. and J.N. are supported by the Spanish project FPA2011-27853-C02-02 and the EU FP7 HadronPhysics3 project. J.N. acknowledges funding by the Deutscher Akademischer Austauschdienst (DAAD), the Fundación Ramón Areces and the hospitality of Bonn and Indiana Universities. A.P.S. is supported in part by the U.S. Department of Energy under Grant DE-FG0287ER40365. J.T.L. is supported by the U.S. National Science Foundation under grant PHY-1205019.

References

[1] R.L. Jaffe, Phys. Rev. D 15 (1977) 267;
R.L. Jaffe, Prog. Theor. Phys. Suppl. 168 (2007) 127;
J.D. Weinstein, N. Isgur, Phys. Rev. Lett. 48 (1982) 659;
U.G. Meissner, Comments Nucl. Part. Phys. 20 (1991) 119;
E. van Beveren, et al., Z. Phys. C 30 (1986) 615;
D. Black, A.H. Fariborz, F. Sannino, J. Schechter, Phys. Rev. D 59 (1999) 074026;
P. Minkowski, W. Ochs, Eur. Phys. J. C 9 (1999) 283;
J.A. Oller, E. Oset, Nucl. Phys. A 620 (1997) 438;
J.A. Oller, E. Oset, Nucl. Phys. A 652 (1999) 407 (Erratum);
E. van Beveren, G. Rupp, Eur. Phys. J. C 22 (2001) 493;
F.E. Close, N.A. Tornqvist, J. Phys. G 28 (2002) R249;
J.R. Pelaez, Phys. Rev. Lett. 92 (2004) 102001;
J. Vijande, A. Valcarce, F. Fernandez, B. Silvestre-Brac, Phys. Rev. D 72 (2005) 034025;
F. Giacosa, Phys. Rev. D 74 (2006) 014028;
L. Maiani, A.D. Polosa, V. Riquer, Phys. Lett. B 651 (2007) 129;
G. 't Hooft, et al., Phys. Lett. B 662 (2008) 424;
T. Hyodo, D. Jido, T. Kunihiro, Nucl. Phys. A 848 (2010) 341.
[2] J.R. Pelaez, G. Rios, Phys. Rev. Lett. 97 (2006) 242002;
J.R. Pelaez, M.R. Pennington, J. Ruiz de Elvira, D.J. Wilson, Phys. Rev. D 84 (2011) 096006.
[3] A.V. Anisovich, V.V. Anisovich, A.V. Sarantsev, Phys. Rev. D 62 (2000) 051502.
[4] P. Masjuan, E. Ruiz Arriola, W. Broniowski, Phys. Rev. D 85 (2012) 094006.
[5] I. Caprini, G. Colangelo, H. Leutwyler, Phys. Rev. Lett. 96 (2006) 132001.
[6] R. Garcia-Martin, R. Kaminski, J.R. Pelaez, J. Ruiz de Elvira, Phys. Rev. Lett. 107 (2011) 072001.
[7] J. Beringer, et al., Particle Data Group, Phys. Rev. D 86 (2012) 010001;
J.R. Pelaez, PoS Confinement X (2012) 019, arXiv:1301.4431 [hep-ph].
[8] G. Epstein, P. Kaus, Phys. Rev. 166 (1968) 1633;
S.-Y. Chu, G. Epstein, P. Kaus, R.C. Slansky, F. Zachariasen, Phys. Rev. 175 (1968) 2098.
[9] P.D.B. Collins, R.C. Johnson, E.J. Squires, Phys. Lett. B 26 (1968) 223.
[10] R. Garcia-Martin, R. Kaminski, J.R. Pelaez, J. Ruiz de Elvira, F.J. Yndurain, Phys. Rev. D 83 (2011) 074004.
[11] J.R. Pelaez, F.J. Yndurain, Phys. Rev. D 69 (2004) 114001.
[12] S. Weinberg, Physica A 96 (1979) 327;
J. Gasser, H. Leutwyler, Ann. Phys. 158 (1984) 142.
[13] C. Lovelace, D. Masson, Nuovo Cimento 26 (1962) 472;
A.O. Barut, F. Calogero, Phys. Rev. 128 (1962) 1383;
A. Ahamadzadeh, P.G. Burke, C. Tate, Phys. Rev. 131 (1963) 1315.